

# Concentration Fluctuations Induced by Orientation Fluctuations in Polymer–Liquid Crystal Mixture

Mikihito Takenaka,\* Hirofumi Shimizu, Shotaro Nishitsuji, and Hirokazu Hasegawa

Department of Polymer Chemistry, Graduate School of Engineering, Kyoto University,  
Kyoto 615-8510, Japan

Received June 26, 2006

**ABSTRACT:** Polymer–liquid crystal (LC) binary mixtures have two modes of concentration fluctuations characterized by the Ornstein–Zernike–Debye form with correlation length  $\xi$  (OZD mode) and Debye–Bueche form with correlation length  $l$  (DB mode) ( $l > \xi$ ) in their one-phase region and isotropic state of LC. The temperature dependence of OZD mode exhibits the critical phenomena similar to common binary mixtures while the DB mode is almost independent of temperature. Under the condition where LC molecules oriented by electric field, the OZD mode is insensitive to the orientation while the DB mode is enhanced perpendicular to the orientation direction. These results indicate that the DB mode is induced by the orientation of LC molecules.

## I. Introduction

The critical phenomena of binary mixtures have been well investigated for decades. We have used scattering experiments to investigate the critical phenomena in the concentration fluctuations of the binary mixtures by measuring the structure factor or scattered intensity. The scattered intensity of the binary mixtures in the one-phase region is described by the Ornstein–Zernike and Debye (OZD) equation, and the analyses with the OZD equation yielded two parameters: the scattered intensity at the scattering vector  $q = 0$ ,  $I(0)$ , and the correlation length,  $\xi$ . Their temperature dependencies are usually described by the 3D Ising model.<sup>1</sup> The critical phenomena of polymer solutions also obey the 3D Ising model.<sup>2</sup> Polymer–liquid crystal (LC) mixtures are kinds of polymer solutions. However, in contrast to other common polymer solutions, polymer–LC mixtures have another order parameter in terms of orientation of the LC molecules in addition to concentration. Thus, the phase behaviors and the critical phenomena of polymer–LC mixtures become more complicated than those in other common polymer solutions. The phase diagrams of polymer–LC mixtures have been investigated extensively. Experimental studies on the phase diagrams have explored that the nematic–isotropic transition of the LC occurs as well as liquid–liquid phase transition between polymer and LC.<sup>3–9</sup> Theoretically, several authors predicted the phase diagrams by combining Flory–Huggins theory for isotropic mixing of two components with Maier–Saupe theory for nematic interactions.<sup>10–12</sup>

Various authors have derived the free energy functional for polymer–LC mixtures by taking into account of spatial concentration and orientation fluctuations and studied the dynamics of phase transition of the LC–polymer mixtures.<sup>7,13–18</sup> They have explored the coupling effects between concentration and orientation fluctuations in the dynamics of phase separation. We can thus expect that the critical phenomena of polymer–LC mixtures are also affected by the coupling effects between concentration and orientation fluctuations.

In this report, we will present the experimental evidence of the existence of concentration fluctuations induced by orientation fluctuations in the critical phenomena of the polymer–LC

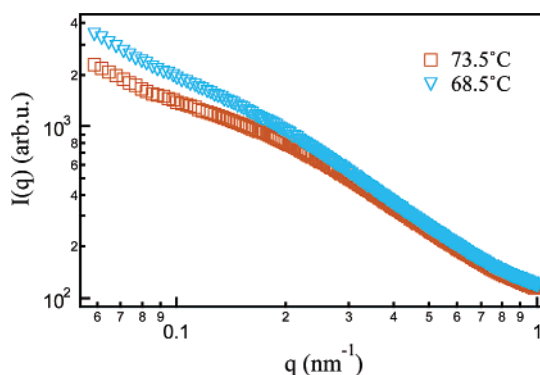


**Figure 1.** Scattered intensity  $I(q)$  is plotted as a function of  $q$  at 73.5 °C (open square) and 68.5 °C (open triangle).

mixture in addition to the concentration fluctuations originating from usual critical phenomena.

## II. Experimental Section

We have investigated the polystyrene (PS)/4-cyano-4'-n-octylbiphenyl (8CB) mixture with small-angle X-ray scattering (SAXS). The weight-averaged molecular weight of PS is  $6.88 \times 10^4$  with a polydispersity index of 1.03. The volume fraction of PS  $\phi_{PS}$  studied here was 0.10, which is near the critical volume fraction in terms of liquid–liquid phase transition. The cloud point of this mixture is 63.5 °C, and the nematic–isotropic transition temperature of 8CB in the mixture is 41.0 °C. It should be noted that the LC is in an isotropic state in one phase of this PS–8CB mixture. SAXS experiments were conducted at the BL45XU, Spring-8.<sup>19</sup> To investigate the effects of the electric field on the concentration fluctuations, we used a cell having a pair of electrodes and sandwiched the sample between the electrodes and measured the scattering pattern under application of 800 V/mm.

## III. Results and Discussion

Figure 1 shows the SAXS scattered intensity  $I(q)$  plotted as a function of the magnitude of the scattering vector  $q [= (4\pi/\lambda) \sin(\theta/2)]$  at 73.5 °C with  $\theta$  and  $\lambda$  being the scattering angle and the wavelength of incident beam. As already mentioned, the scattered intensity of polymer solutions should be well described by the OZD equation. However, the scattered intensity of PS–8CB exhibits an upturn at  $q < 0.09 \text{ nm}^{-1}$  and cannot be described by the OZD form alone. The upturn at lower  $q$  region

\* To whom correspondence should be addressed.

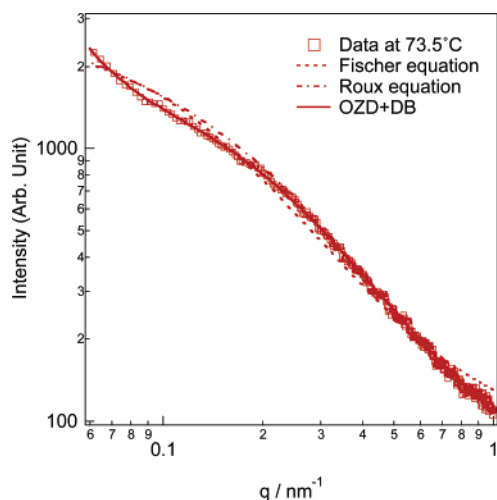


**Figure 2.** (a) Fitting results with three model equations for  $I(q)$  at 73.5 °C. Broken, dash-dotted, and solid lines correspond to the fitting results with Fischer equation (eq 1), Roux equation (eq 3), and DB + OZD equation (eq 4), respectively.

suggests the existence of larger concentration fluctuations in addition to the concentration fluctuations caused by the osmotic compressibility. This kind of unusual excess scattering has been observed in glass-forming liquids,<sup>20,21</sup> polymer melts,<sup>22</sup> and a polymer solution.<sup>23</sup> For glass-forming liquids, the origin of excess scattering is Fischer's cluster, and the excess scattering can be described by the following scattering function introducing a fractal dimension  $D$ :<sup>20,21</sup>

$$I(q) = I(0)q^{-1}(q^2 + \xi^{-2})^{(1-D)/2} \arctan(q\xi) + I_{\text{TDS}} \quad (1)$$

where  $K$  and  $\xi$  are respectively a constant and correlation length for density.  $I_{\text{TDS}}$  is the thermal diffuse scattering of the mixture. This generalized density scattering function (Fischer equation) is the Fourier transform of the correlation function

$$g(r) = \frac{a}{r^{3-D}} \exp\left(-\frac{\xi}{r}\right) \quad (2)$$

First we tried to analyze the scattering function with the Fischer equation. The broken line in Figure 2 shows the results of nonlinear regression with eq 1 having  $\xi$ ,  $D$ , and  $I_{\text{TDS}}$  as floating parameters. Although the fitting yielded  $K = 29.0$ ,  $\xi = 9.1$  nm, and  $D = 2.0$ , the Fischer equation cannot describe the upturn at the low  $q$  region.

Next, we tried to the scattering function derived by Roux et al. Roux et al. derived the scattering function derived from Landau–Ginzburg theory using two coupled order parameters,  $\rho$  and  $\eta$ , to describe the scattering function of the sponge phase of surfactant solutions.<sup>24</sup> The result is

$$I(q) = \frac{I_\rho(0)}{(1 + q^2\xi_\rho^2)} + I_\eta(0) \frac{(1 + q^2\xi_c^2)^2 \arctan(q\xi_\eta/2)}{(1 + q^2\xi_\rho^2)^2 (q\xi_\eta/2)} + I_{\text{TDS}} \quad (3)$$

where  $\xi_\rho$  and  $\xi_\eta$  are correlation length for order parameter  $\rho$  and  $\eta$ , respectively, and  $\xi_c$  is the correlation length due to gradient coupling between  $\rho$  and  $\eta$ . In PS–8CB, there are two kinds of order parameters: the concentration fluctuations between PS and LC and the orientation fluctuations of LC, as the sponge phase of surfactant solutions. Thus, we can anticipate eq 3 (Roux equation) can well describe the scattering function of PS–8CB. The dotted line in Figure 2 indicates the fitting

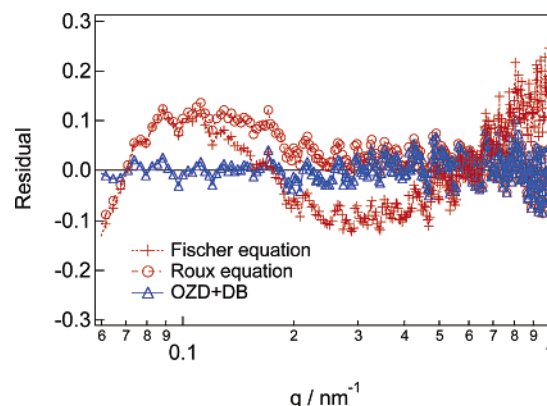


**Figure 3.** Residuals of the fitting results for the three models are plotted as a function of  $q$ . Cross, open circle, and open triangle correspond to the fitting results with Fischer equation (eq 1), Roux equation (eq 3), and DB + OZD equation (eq 4), respectively.

result of Roux equation with  $I_\rho(0) = 1.51 \times 10^3$ ,  $\xi_\rho = 5.11$  nm,  $I_\eta(0) = 8.67 \times 10^3$ ,  $\xi_c = 0.150$  nm,  $\xi_\eta = 5.69 \times 10^2$  nm, and  $I_{\text{TDS}} = 52.3$ . The fitting result is better than that of the Fischer equation. However, the fitting result around the upturn region is still not good. This is because the upturn region exhibits the strong correlation as shown in much steeper decay around the upturn region. Thus, we employed the Debye–Buche (DB) equation to express the upturn region, and we assumed that the scattering profiles are described by the following linear combination of the Debye–Buche (DB) equation and OZD equation:

$$I(q) = \frac{I_{\text{DB}}(0)}{(1 + q^2l^2)^2} + \frac{I_{\text{OZD}}(0)}{1 + q^2\xi^2} + I_{\text{TDS}} \quad (4)$$

where  $l$  and  $\xi$  are correlation length for DB and OZD equations, respectively. We fitted the experimental data by eq 4 with  $I_{\text{DB}}(0)$ ,  $l$ ,  $I_{\text{OZD}}(0)$ ,  $\xi$ , and  $I_{\text{TDS}}$  being floating parameters. The solid line in Figure 2 is the fitting result with  $I_{\text{DB}}(0) = 6.90 \times 10^4$ ,  $l = 46.7$  nm,  $I_{\text{OZD}}(0) = 1.52 \times 10^3$ ,  $\xi = 5.12$  nm, and  $I_{\text{TDS}} = 52.8$  and shows eq 4 can describe the experimental results better than equation. As shown in Figure 3, the residual of the fitting result for eq 4 is better than those for eqs 1 and 3. Thus, we analyzed the data by using eq 4 for further analyses. The temperature dependencies of each parameter obtained by fitting are shown in Figure 4. We found the critical phenomena in the parameters  $I_{\text{OZD}}(0)$  and  $\xi$ . Namely,  $I_{\text{OZD}}(0)$  and  $\xi$  are expressed by the following equations:

$$\xi \sim (T - T_S)^{-0.62} \quad (5)$$

$$I_{\text{OZD}}(0) \sim (T - T_S)^{-1.24} \quad (6)$$

where  $T_S$  is the spinodal temperature of PS–8CB and is estimated to be 59.6 °C. Thus, the concentration fluctuations expressed by the OZD equation (OZD mode) originate from the osmotic compressibility of the PS–8CB mixture. On the other hand,  $I_{\text{DB}}(0)$  and  $l$  do not show any critical phenomena, and both  $I_{\text{DB}}(0)$  and  $l$  are almost independent of temperature, as shown in Figure 4b. This indicates that the concentration fluctuations expressed by DB equation (DB mode) at smaller  $q$  or larger wavelength are independent of the osmotic compressibility. We assume that the orientation fluctuations of LC molecules may induce the DB mode of the concentration fluctuations. Thus, we applied an electric field to the PS–8CB and investigated how the electric field affects the concentration fluctuations. The electric field induces the alignment of the LC molecules along the electric field, and we can expect that the

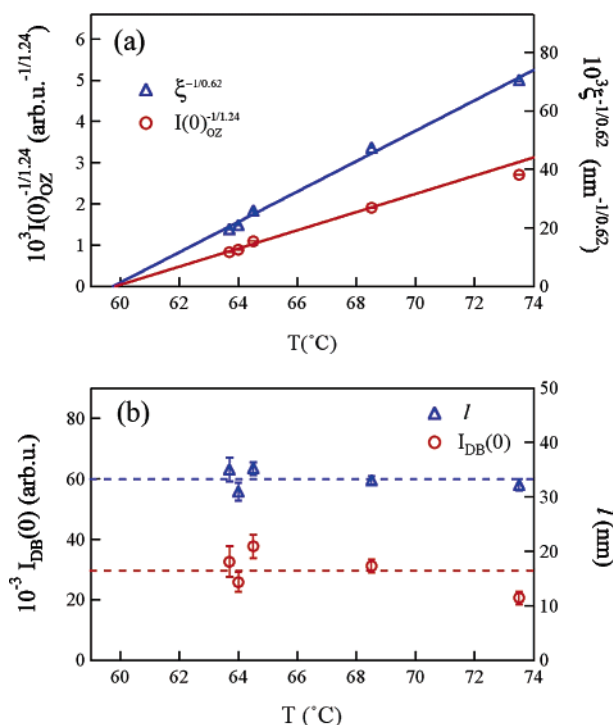


**Figure 4.** (a)  $I_{\text{OZD}}(0) \sim (T - T_s)^{-1/1.24}$  (open triangle) and  $\xi^{-1/0.62}$  (open circle) are plotted as a function of  $T$ . The linear relationship in the plots indicates that the temperature dependencies of  $I_{\text{OZD}}(0)$  and  $\xi$  can be described by the 3D Ising model. The lines merge at  $T_s = 59.6$  °C on the  $T$ -axis. Error bars become within symbols. (b) Temperature dependence of  $I_{\text{DB}}(0)$  (open triangle) and  $l$  (open circle).  $I_{\text{DB}}(0)$  and  $l$  do not show critical phenomena. Broken lines are guides for eyes.

DB modes become anisotropic if the orientation fluctuations affect the concentration fluctuations.

Figure 5 shows the effects of the electric field on the 2-dimensional SAXS patterns of the PS–8CB. The scattering pattern at 0 V/mm is isotropic while the scattering pattern at 800 V/mm is elongated perpendicular to the electric field direction, indicating that the electric field enhances the concentration fluctuations perpendicular to its direction. This enhancement is due to the alignment of the orientation of 8CB molecules. Figure 6 shows the scattered intensity  $I_{\parallel}(q)$  parallel to the electric field and  $I_{\perp}(q)$  perpendicular to the electric field direction at 73.5 °C and 800 V/mm as a function of  $q$ . We also plotted the scattered intensity  $I_0(q)$  at 0 V/mm in the same figure. As for  $I_{\perp}(q)$ , the enhancement of the scattered intensity is

observed in  $I_{\perp}(q)$  at  $q < 0.09 \text{ nm}^{-1}$ , while  $I_{\perp}(q)$  is almost identical with  $I_0(q)$  at  $q > 0.09 \text{ nm}^{-1}$ . Each solid line is the fitting result of experimental data with eq 4. The fitting results yielded  $l_{\perp} = 37.3 \pm 1.4 \text{ nm}$ ,  $l_{\parallel} = 30.7 \pm 1.3 \text{ nm}$ ,  $l_0 = 29.8 \pm 1.1 \text{ nm}$ ,  $\xi_{\perp} = 5.0 \pm 0.1 \text{ nm}$ ,  $\xi_{\parallel} = 4.9 \pm 0.1 \text{ nm}$ , and  $\xi_0 = 5.0 \pm 0.1 \text{ nm}$ , where  $\perp$ ,  $\parallel$ , and 0 denote perpendicular, parallel, and 0 V/min, respectively.  $l_{\perp}$  is larger than  $l_{\parallel} \cong l_0$  while  $\xi$  is independent of the electric field, indicating that the DB mode perpendicular to the electric field is enhanced but that the OZD mode is insensitive to the electric field. This enhancement is proof that the DB mode originates from the orientation fluctuations of the LC molecules.

SAXS intensity depends on the electron density difference, and the orientation fluctuations themselves cause the electron density fluctuations since volume per one LC molecule depends on its orientation, such as the electron density difference between amorphous and crystalline regions in crystalline polymers. We can derive the correlation or scattering function for orientation fluctuations from free energy functional:<sup>7</sup>

$$S_s(q) = \frac{S_s(0)}{1 + \kappa^2 q^2} \quad (7)$$

Here  $\kappa$  is the correlation length for orientation fluctuations defined by

$$\kappa = \left( \frac{L_1 + 2L_2/3}{f_{ss}} \right)^{1/2} \quad (8)$$

where  $L_1 = b^2/8$ ,  $L_2 = b^2/2$ , and  $f_{ss}$  is the second derivative of free energy and equal to  $1 - T_{\text{NI}}/T$ , with  $b$  and  $T_{\text{NI}}$  being the molecular size of a LC and the nematic–isotropic temperature of the LC.<sup>14</sup> Substituting  $b = 2 \text{ nm}$ ,  $T_{\text{NI}} = 315 \text{ K}$ , and  $T = 346 \text{ K}$ , we obtained  $\kappa = 4.5 \text{ nm}$ . This value is much smaller than  $l_0 = 29.8 \text{ nm}$ . Moreover, the scattering function is OZD form and does not agree with DB form obtained experimentally. Thus, we need to consider another effects induced by orientation fluctuations. We speculate that the larger scale concentration fluctuations may be induced by orientation fluctuations. Matsuyama has calculated the polymer swelling ratio in polymer–LC mixtures as a function of the oriental dependent interactions between LC molecules under good solvent condition.<sup>25</sup> He found that a flexible polymer condensed with the oriental dependent interactions (please see Figure 2 in ref 25). Thus, even though orientation fluctuations is activated thermally, the orientation fluctuations, where the orientation interaction is increased,

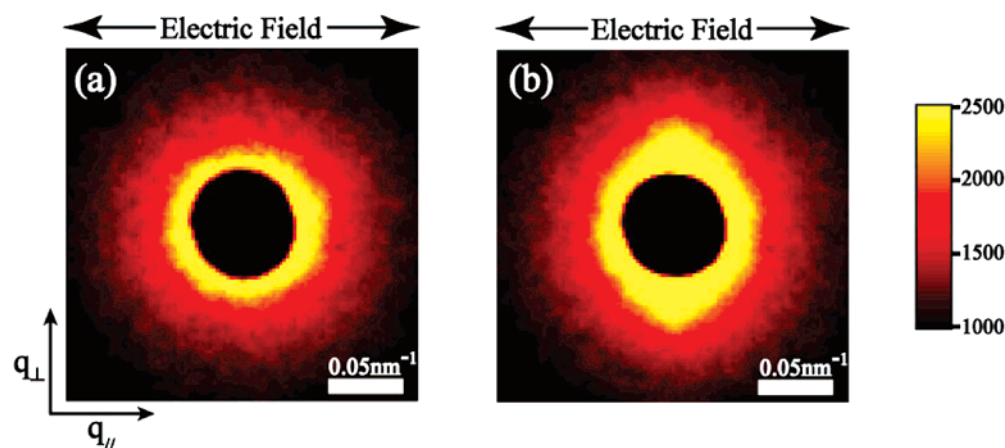


**Figure 5.** Two-dimensional SAXS patterns of the PS–8CB at 0 (a) and 800 V/mm (b). The direction of the electric field is indicated by the arrow. The scattering pattern at 0 V/mm is isotropic while the scattering pattern at 800 V/mm is elongated in the direction perpendicular to the electric field.

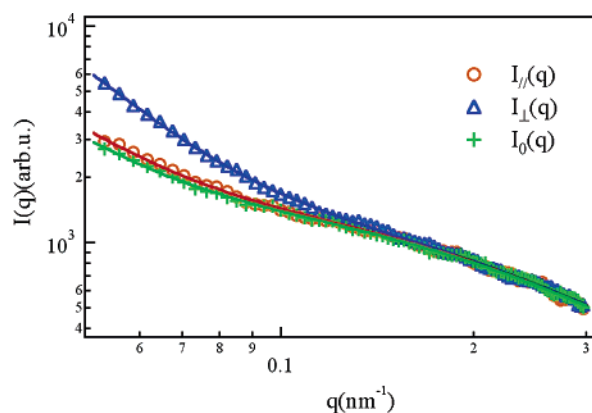


**Figure 6.** Scattered intensity  $I_{||}(q)$  (open circle) parallel to the electric field and that  $I_{\perp}(q)$  (open triangle) perpendicular to the electric field at 73.5 °C and 800 V/mm are plotted as a function of  $q$ . The cross symbol indicates the scattered intensity  $I_0(q)$  at 73.5 °C and 0 V/mm. The solid curves correspond to the fitting with eq 4.

possibly expel polymer chains from the LC-rich region so that the concentration fluctuations are induced by the orientation fluctuations. This exclusion effect can explain the anisotropic enhancement of concentration fluctuations perpendicular to the electric field since the attractive interaction perpendicular to the alignment direction of LC molecules is stronger than that parallel to the alignment direction. Further consideration of the coupling between the concentration and orientation fluctuations in critical phenomena in polymer–LC mixtures will be needed.

#### IV. Conclusion

We have investigated the critical phenomena of polymer–LC mixtures which are also affected by the coupling effects between concentration and orientation fluctuations. Polymer–LC binary mixtures have two modes of concentration fluctuations characterized by OZD mode with correlation length  $\xi$  and DB mode with correlation length  $l$  in their one-phase region and isotropic state of LC. The temperature dependence of the OZD mode exhibits the critical phenomena similar to common binary mixtures while the DB mode is almost independent of temperature. Under the condition where LC molecules oriented by electric field, the OZD mode is insensitive to the orientation while the DB mode is enhanced perpendicular to the orientation direction. We calculated the correlation length induced by orientation fluctuations of LC itself from the free energy functional of polymer–LC systems and found the calculated

correlation length is much shorter than the experimental results. These results indicate that the DB mode is induced by the orientation of LC molecules. It should be noted that unusual concentration fluctuations with large scale have been found in poly(ethylene oxide)–water solution by Devanand and Selser.<sup>23</sup> However, the origin of the unusual concentration fluctuations is the long-range interaction between interpolymer and/or intrapolymer. On the other hand, the origin of the unusual concentration fluctuations in PS–8CB is the coupling between these density fluctuations and the orientational fluctuations associated with the liquid crystal solvent.

#### References and Notes

- (1) Stanley, H. E. *Introduction to Phase Transitions and Critical Phenomena*; Oxford UP: London, 1971.
- (2) Kuwahara, N.; Fenby, D. V.; Tamsky, M.; Chu, B. *J. Chem. Phys.* **1971**, *55*, 1140.
- (3) Ahn, W.; Kim, C. Y.; Kim, H.; Kim, S. C. *Macromolecules* **1992**, *25*, 5002.
- (4) Benmouna, F.; Daoudi, A.; Roussel, F.; Leclercq, L.; Buisine, J. M.; Coqueret, X.; Benmouna, M.; Ewen, B.; Maschke, U. *Macromolecules* **2000**, *33*, 960.
- (5) Dubault, A.; Casagrande, C.; Veysie, M.; Deloche, B. *Phys. Rev. Lett.* **1980**, *45*, 1645.
- (6) Kronberg, B.; Bassignana, I.; Patterson, D. J. *Phys. Chem.* **1978**, *82*, 1714.
- (7) Matsuyama, A.; Evans, R. M. L.; Cates, M. E. *Phys. Rev. E* **2000**, *61*, 2977.
- (8) Shen, C. S.; Kyu, T. *J. Chem. Phys.* **1995**, *102*, 556.
- (9) Smith, G. W. *Phys. Rev. Lett.* **1993**, *70*, 198.
- (10) Holyst, R.; Schick, M. *J. Chem. Phys.* **1992**, *96*, 721.
- (11) Matsuyama, A.; Kato, T. *J. Chem. Phys.* **1996**, *105*, 1654.
- (12) Benmouna, F.; Bedjaoui, L.; Maschke, U.; Coqueret, X.; Benmouna, M. *Macromol. Theory Simul.* **1998**, *7*, 599.
- (13) Araki, T.; Tanaka, H. *Phys. Rev. Lett.* **2004**, *93*.
- (14) Fukuda, J. *Eur. Phys. J. B* **1999**, *7*, 573.
- (15) Fukuda, J. *Phys. Rev. E* **1999**, *59*, 3275.
- (16) Lapena, A. M.; Glotzer, S. C.; Langer, S. A.; Liu, A. J. *Phys. Rev. E* **1999**, *60*, R29.
- (17) Liu, A. J.; Fredrickson, G. H. *Macromolecules* **1996**, *29*, 8000.
- (18) Liu, A. J.; Fredrickson, G. H. *Macromolecules* **1993**, *26*, 2817.
- (19) Fujisawa, T.; Inoue, K.; Oka, T.; Iwamoto, H.; Uruga, T.; Kumasaka, T.; Inoko, Y.; Yagi, N.; Yamamoto, M.; Ueki, T. *J. Appl. Crystallogr.* **2000**, *33*, 797.
- (20) Bakai, A. S.; Fischer, E. W. *J. Chem. Phys.* **2004**, *120*, 5235.
- (21) Patkowski, A.; Fischer, E. W.; Steffen, W.; Glaser, H.; Baumann, M.; Ruths, T.; Meier, G. *Phys. Rev. E* **2001**, *63*, art. no.
- (22) Walkenhorst, R.; Selser, J. C.; Piet, G. *J. Chem. Phys.* **1998**, *109*, 11043.
- (23) Devanand, K.; Selser, J. C. *Macromolecules* **1991**, *24*, 5943.
- (24) Roux, D.; Coulon, C.; Cates, M. E. *J. Phys. Chem.* **1992**, *96*, 4174.
- (25) Matsuyama, A. *Phys. Rev. E* **2003**, *67*.

MA061427E